COMPDYN 2013
4th ECCOMAS Thematic Conference on
Computational Methods in Structural Dynamics and Earthquake Engineering
M. Papadrakakis, V. Papadopoulos, V. Plevris (eds.)
Kos Island, Greece, 12–14June 2013

# STRUCTURAL ANALYSIS OF MULTISTORY BUILDING USING COUPLED BEM-STIFFNESS MATRIX

**RAMIZ W. MOHAREB[1], YOUSSEF F. RASHED[1]*, MINA WAGDY[2], MOSTAFA E. MOBASHER[1,3]**

1 Dept. of Structural Engineering, Cairo University, Giza, Egypt.

enramiz@yahoo.com, youssef@eng.cu.edu.eg

2 Dar Al-handasah consultant, department of structures, Dokki, Giza, Egypt.

mina.wagdy@dargroup.com

3 Civil Engineering Department, British University in Egypt, Sherouk, Egypt.

mostafa.mobasher@bue.edu.eg

**Keywords:** Boundary element method, multi-storey building, lateral analysis, matrix analysis.

**Abstract.** *This paper presents a structural analysis scheme for multistory buildings. In this analysis the boundary element method (BEM) is used to derive the stiffness. Such a matrix is coupled with the vertical skeletal elements using the traditional assembly procedures. Nodal displacements and end-forces are then computed, hence, post-processing is done for frame and floor elements. The results are compared against results of traditional finite element analysis.*

## 1 INTRODUCTION

Over the past decades, high-rise buildings became a part of the daily structural engineering practice. In high-rise buildings, the effects of lateral loads e.g seismic and wind loads are critical; they have to be considered in the structural analysis process.

Several methods were implemented to perform structural analysis of structures due to lateral loading. Initially, the simple structural geometry allowed simple manual calculations to provide a good enough solution [1]. The traditional Moment Distribution method and Matrix Analysis of structures were applied to regular framed structures. Many researches contributed to the techniques of modeling the irregular vertical elements (shear walls and cores). Some efforts presented analytical solutions via presenting a solution to partial differential equations [2]. Other solutions were based on numerical modeling of walls.

The increasing complexity of the geometries increased the difficulty of the implementation of manual calculations leading to a need for more flexible numerical techniques. Hence, the finite element method [3] started to present itself as a convenient solution for structural analysis problems. The flexibility of the finite element method allows the modeling of any floor shape, hence, get its stiffness matrix. A typical finite element model of a structure gets the stiffness of the floor as a two-dimensional element, either shell or plate, and assembles it with stiffness matrix of vertical elements modeled as one-dimensional element.

The finite element modeling of structures passed through many development stages. Works in [2-5] presented improved and more efficient modeling schemes to deal with tall structures containing coupled shear walls and cores. Improvements included reduction in computational effort and reduced numerical errors. Other models were concerned with the modeling of coupling beams as continuous connections; this is based on the high in-plane stiffness of horizontal floors. The impacts of the variations of the walls' cross-sections along the building's height were considered in [6-13].

In this paper a new scheme for the lateral analysis of structures is presented. The scheme is based on computerized matrix analysis of structures. The floor stiffness matrix is derived from a boundary element formulation; the floor stiffness matrix is condensed at the frame nodes. The stiffness matrices of columns are computed as one dimensional element. The stiffness matrices of complex wall shapes are computed as one dimensional element, however, the twisting behavior is included via adding warping degrees of freedom. The boundary element model of plates and the boundary element computation of warping functions for frames are reviewed. The computation of stiffness matrices and solution of equations is explained. Numerical examples are provided to illustrate the validity and efficiency of the proposed analysis scheme.

## 2 BEM APPLIED

This section reviews the boundary elements mathematical models that are utilized in the proposed analysis scheme. The first section, Section 2.1, reviews the boundary element analysis model for shear deformable plates. This model is the basis for the derivation of the plate stiffness matrix presented in Section 3. The second section,

Section 2.2, reviews the boundary element model implemented to calculate the warping functions and its derivatives for vertical supporting element cross sections. These values are required in the computation of the stiffness matrices of vertical elements presented in Section 4.

## 2.1 BEM for Plates

The problem of flat plates rested on column was studied by Rashed [14]. His work was done using the shear deformable thick plate theory. Columns or internal walls are modeled using internal supporting cells with the real geometry of the cross section. Three generalized forces are considered at each internal support: two bending moments in two directions as well as shear force in the vertical direction. These generalized forces are considered to vary constantly over the column cross-section.

The work presented herein uses the shear deformable plate bending theory according to Reissner's[15,16].In this section a review of this theory is outlined. Greek indices vary from 1 to 2 whereas; Roman indices vary from 1 to 3. The comma subscript is used to denote differentiation.

Consider a typical flat slab as in Figure 2.1, the boundary integral equation may be written as follows:

$$C_{ij}(\xi)u_j(\xi)+\int_{\Gamma(y)} T_{ij}(y,\xi)u_j(y)\,d\Gamma(y)=\int_{\Gamma(y)} U_{ij}(y,\xi)t_j(y)\,d\Gamma(y)$$

$$+\sum_c\{\int_{\Omega_c(c)}[U_{ik}(\xi,c)-\frac{\nu}{(1-\nu)\lambda^2}U_{i\alpha,\alpha}(\xi,c)\delta_{3k}]F_k(c)d\Omega_c(c)\} \qquad (1)$$

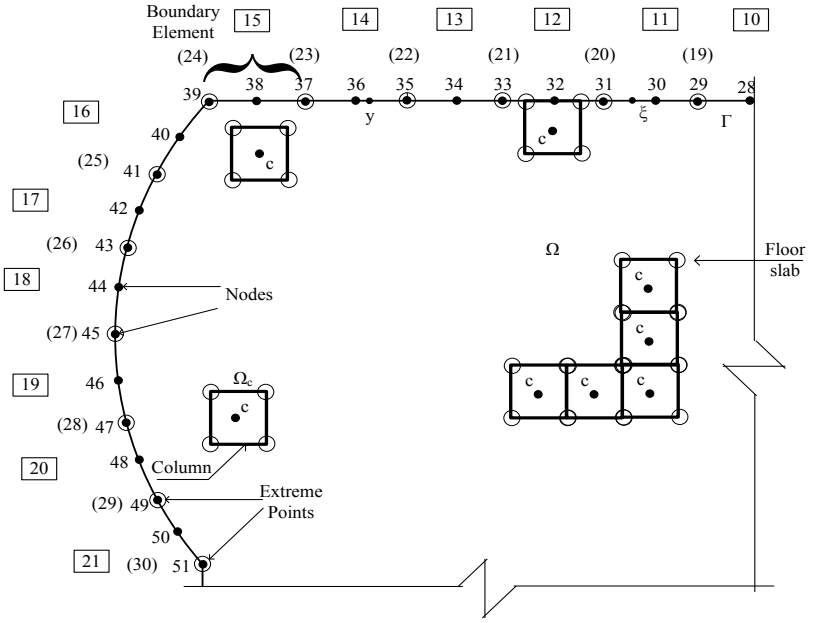


Figure 2.1: Geometry and boundary element discretization for a typical flat slab.

In which $U^*_{ij}(\xi,y)$ denotes a two-point kernel which represents the value of the generalized displacement in the j direction at a field point (y) due to a unit pulse (load) in

the *i* direction located at a source point $\xi_k$ .The boundary traction fundamental solution $T_{ij}^{*}(\xi, y)$ .The column reactions are denoted by $F_k(c)$ .

Equation (1) represents 3 equations in 6 unknowns. In order to solve the previous problem, a collocation scheme is carried out at each internal column center. This equation is as follows Rashed [14]:

$$u_i(c) + \int_{\Gamma} T_{ij}(c, y) u_j(\mathrm{y}) d\Gamma(\mathrm{y}) = \int_{\Gamma} U_{ij}(c, y) t_j(\mathrm{y}) d\Gamma(\mathrm{y})$$

$$+ \sum_{c} \left\{ \int_{\Omega_c(c)} [U_{ik}(\xi, c) - \frac{\nu}{(1-\nu)\lambda^2} U_{i\alpha,\alpha}(\xi, c)\delta_{3k}] F_k(c) d\Omega_c(c) \right\}$$

$$\times \left[ \frac{-u_k(c) S_k(c)}{A(c)} \right] \qquad (2)$$

Where: c is a new source point located at each column center. This final equation provides additional three equations. Solving eq. (1) together with eq. (2), the values of the unknown boundary generalized tractions and displacement together with the column internal generalized displacement and tractions can be determined.

## 2.2 BEM for warping

In this section torsion analysis of sections is reviewed. Warping effects must be considered at designing core elements. Vlasov [17] was one of the leading developers of theory for warping torsion. The equations devised in [17] are used herein.

Consider an arbitrary cross-section twisted by moments Mt applied at its ends as shown in Figure 2-2. This torsion moment is considered constant over the length of the element. Saint venant torsion **Error! Reference source not found.**18] assumed, at any point A(x1, x2, x3), the displacements *u1* and *u 2*.

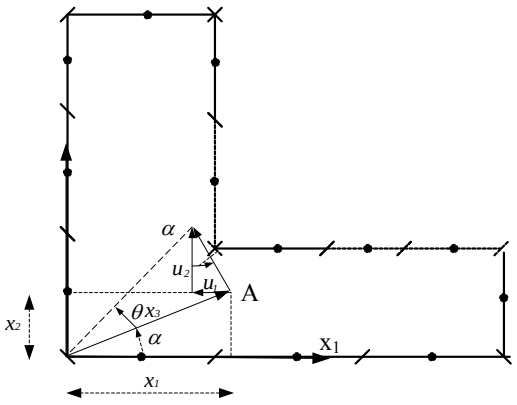


Figure 2-2 Displacement components in a cross-section of a twisted bar.

In order to obtain the boundary integral of the problem, any standard procedure such as suitable integral identity can be used. The final equation can take the form:

$$\phi(\xi) + \int_{\Gamma} \frac{\partial u^*}{\partial n_q} \phi(\mathrm{y}) d\Gamma = \int_{\Gamma} U^*(\xi, \mathrm{y}) \frac{\partial \phi}{\partial n} d\Gamma \tag{3}$$

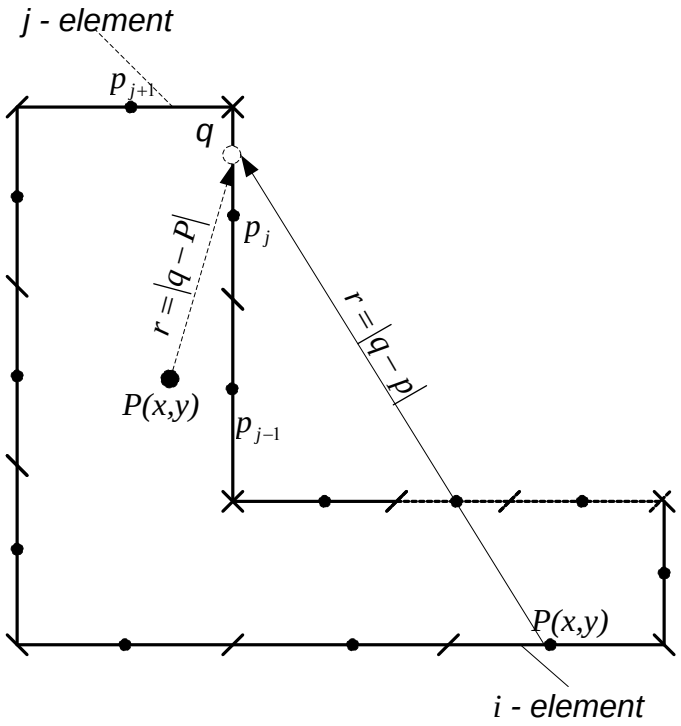


Figure 2-3 Nodal-point location and relative distances for constant element discretization.

The domain integral is transformed to the boundary integral form as follow:

$$\frac{1}{2}\phi(\xi) = -\int_{\Gamma} \left[ U^*(\xi, \mathrm{y}) - u(\xi) \frac{\partial U^*(\xi, \mathrm{y})}{\partial n_q} \right] ds_q \tag{4}$$

The boundary $\Gamma$ is discretized into N constant elements. The values of the boundary quantity $\phi$ and its normal derivative $\partial\phi/\partial n$ are assumed constant over each element and equal to their value at the mid-point of the element.

The discretized form of eq. (4) is expressed for a given point p, on $\Gamma$ as

$$\frac{1}{2}\phi^i(\xi) = -\sum_{j=1}^{N} \int_{\Gamma} U^*(\xi, \mathrm{y}) \frac{\partial U^*(y)}{\partial n_q} ds_q + \sum_{j=1}^{N} \int_{\Gamma} u(y) \frac{\partial U^*(\xi, \mathrm{y})}{\partial n_q} ds_q \tag{5}$$

Where: $\Gamma$ is the segment (straight line) on which the j-$^{th}$ node is located and over which integration is carried out.

Denoted the coefficients $\hat{H}_{ij}$ and $G_{ij}$ are defined as:

$$\hat{H}_{ij} = \int_{\Gamma} \frac{\partial U^*(\xi, \mathrm{y})}{\partial n_q} ds \tag{6}$$

$$G_{ij} = \int_{\Gamma} U^*(\xi, \mathrm{y}) ds \tag{7}$$

Introducing the notation (6) and (7) into eq. (5), the discrete form of the solution becomes

$$\frac{1}{2}u^i + \sum_{j=1}^{N} \widehat{H}_{ij} u^j = \sum_{j=1}^{N} G_{ij} u_n^j \tag{8}$$

$$H_{ij} = \widehat{H}_{ij} - \frac{1}{2}\delta_{ij} \tag{9}$$

Eq. (2.78) may further be written as

$$\sum_{j=1}^{N} H_{ij} u^j = \sum_{j=1}^{N} G_{ij} u_n^j \tag{10}$$

The solution $\phi$ can be computed at any point y in the domain $\Omega$ by virtue of eq. (4). Applying the same discretization as in eq. (5), we arrive at the following expression:

$$u(y) = \sum_{j=1}^{N} \widehat{H}_{ij} u^j - \sum_{j=1}^{N} G_{ij} u_n^j \tag{11}$$

The coefficients $G_{ij}$ and $\widehat{H}_{ij}$ are computed again from the integrals, but in this case the boundary point pi, is replaced in the expressions by the field point P in $\Omega$.

## 3 PLATE STIFFNESS MATRIX

After discretizing the plate boundary to NE quadratic boundary elements, equation (1) could be re-written in a matrix form as follows:

$$[[A]_{3N\times 3N} \quad [A_2]_{3N\times 3N_c}] \begin{Bmatrix} \{u/t\}_{3N\times 1} \\ \{F\}_{3N_c\times 1} \end{Bmatrix} = \{RHS_b\}_{3N\times 1} \tag{12}$$

Combining equation (2)after discretization together with equation (1)gives:

$$\begin{bmatrix} [A]_{3N\times 3N} & [A_2]_{3N\times 3N_c} & [0]_{3N\times 3N_c} \\ [A_1]_{3N_c\times 3N} & [A_3]_{3N_c\times 3N_c} & [I]_{3N_c\times 3N_c} \end{bmatrix} \begin{Bmatrix} \{u/t\}_{3N\times 1} \\ \{F\}_{3N_c\times 1} \\ \{u_c\}_{3N_c\times 1} \end{Bmatrix} = \begin{Bmatrix} \{RHS_b\}_{3N\times 1} \\ \{RHS_c\}_{3N_c\times 1} \end{Bmatrix} \tag{13}$$

If the support elements are considered to have a free edge and no internal loading, considered equation (13) could be re-written as follows after placing the $\{u_c\}$vector on its right hand side:

$$\begin{bmatrix} [A]_{3N\times 3N} & [A_2]_{3N\times 3N_c} & [0]_{3N\times 3N_c} \\ [A_1]_{3N_c\times 3N} & [A_3]_{3N_c\times 3N_c} & [I]_{3N_c\times 3N_c} \end{bmatrix} \begin{Bmatrix} \{u\}_{3N\times 1} \\ \{F\}_{3N_c\times 1} \end{Bmatrix} = -\begin{Bmatrix} \{0\}_{3N\times 1} \\ \{u_c\}_{3N_c\times 1} \end{Bmatrix} \tag{14}$$

If different cases of loading are considered such that the number of load cases is chosen to be equal to 3Nc, hence equation (14) could be re-written as follows:

(15)

$$\begin{bmatrix} [A]_{3N\times 3N} & [A_2]_{3N\times 3N_c} & [0]_{3N\times 3N_c} \\ [A_1]_{3N_c\times 3N} & [A_3]_{3N_c\times 3N_c} & [I]_{3N_c\times 3N_c} \end{bmatrix} \begin{bmatrix} [u]_{3N\times 3N_c} \\ [F]_{3N_c\times 3N_c} \end{bmatrix} = -\begin{bmatrix} [0]_{3N\times 3N_c} \\ [u_c]_{3N_c\times 3N_c} \end{bmatrix}$$

In order to force the force matrix $[F]$ to represent the slab stiffness matrix $[K]$ corresponding to the previously degrees of freedom, $[u_c]$ should be set to the identity matrix $[I]$. Therefore equation (14) could be rewritten as follows:

$$\begin{bmatrix} [A]_{3N\times 3N} & [A_2]_{3N\times 3N_c} \\ [A_1]_{3N_c\times 3N} & [A_3]_{3N_c\times 3N_c} \end{bmatrix} \begin{bmatrix} [u]_{3N\times 3N_c} \\ [K]_{3N_c\times 3N_c} \end{bmatrix} = -\begin{bmatrix} [0]_{3N\times 3N_c} \\ [I]_{3N_c\times 3N_c} \end{bmatrix} \quad (15)$$

Rearranging equation (14) to give:

$$\begin{bmatrix} [u]_{3N\times 3N_c} \\ [K]_{3N_c\times 3N_c} \end{bmatrix} = -\begin{bmatrix} [A]_{3N\times 3N} & [A_2]_{3N\times 3N_c} \\ [A_1]_{3N_c\times 3N} & [A_3]_{3N_c\times 3N_c} \end{bmatrix}^{-1} \begin{bmatrix} [0]_{3N\times 3N_c} \\ [I]_{3N_c\times 3N_c} \end{bmatrix} \quad (16)$$

Equation (16) could be used to obtain the stiffness matrix of the slab panel at the corresponding degrees of freedom defined at column positions.

## 4 FRAME STIFFNESS MATRIX

he stiffness atri [ c of vertical elements not including warping effects is defined by:

$$\left[\overline{\mathrm{K}}_{\mathrm{c}}\right]_{12\times 12} = \left[T_D\right]_{12\times 12}\left[R\right]_{12\times 12}\left[K_c^*\right]_{12\times 12}\left[R\right]^T_{12\times 12}\left[C_D\right]^{-1}_{12\times 12} \quad (17)$$

he stiffness atri [ cw] of vertical elements including warping effects is defined by:

$$\left[\overline{\mathrm{K}}_{\mathrm{cw}}\right]_{14\times 14} = \left[T_{Dw}\right]_{14\times 14}\left[R_w\right]_{14\times 14}\left[K_{cw}^*\right]_{14\times 14}\left[R_w\right]^T_{14\times 14}\left[C_{Dw}\right]^{-1}_{14\times 14} \quad (18)$$

Where $\left[K_c^*\right]$ is the local frame element stiffness matrix, [R] is the 3D transformation matrix, $\left[T_D\right]$ and $\left[C_D\right]$ are transformation matrices that change the position the degrees of the in-plane degrees of freedom to the plate master joint to apply the slab diaphragm effect[2 . he subscript “w” denotes a trices related to warping walls. The computation of warping functions and derivatives are based on [18].

# 5 NUMERICAL EXAMPLES

## 5.1 Example (1):Slab resting on three columns

The purpose of this example is to compute the lateral drift of a single story building by the proposed method, hence, a comparison is made between the present results to those of the finite element method. Three numerical models are considered, two are based on the finite element method (FEM) and the third one is based on the proposed method. A comparison is carried out for the computed drift of a twenty story building has a similar floor slab as that of the one-story building. A parametric study is carried out to study the effect of the real geometric properties of the connecting cross sectional area of the vertical supporting element to the slab. The slab has a thickness of 0.2 m, and dimensions of 4×4m. Column dimensions are 0.5×0.5m as shown in Figure 5-1. The slab material has a modulus of elasticity equal to 2210000 t/m2 and Poisson's ratio of 0.2.The columns modulus of elasticity is equal to 2210000 t/m2. A 10t is applied in the X direction at co-ordinates x=0, y=2 m at the level of the slab. The considered height of the story is 3m.

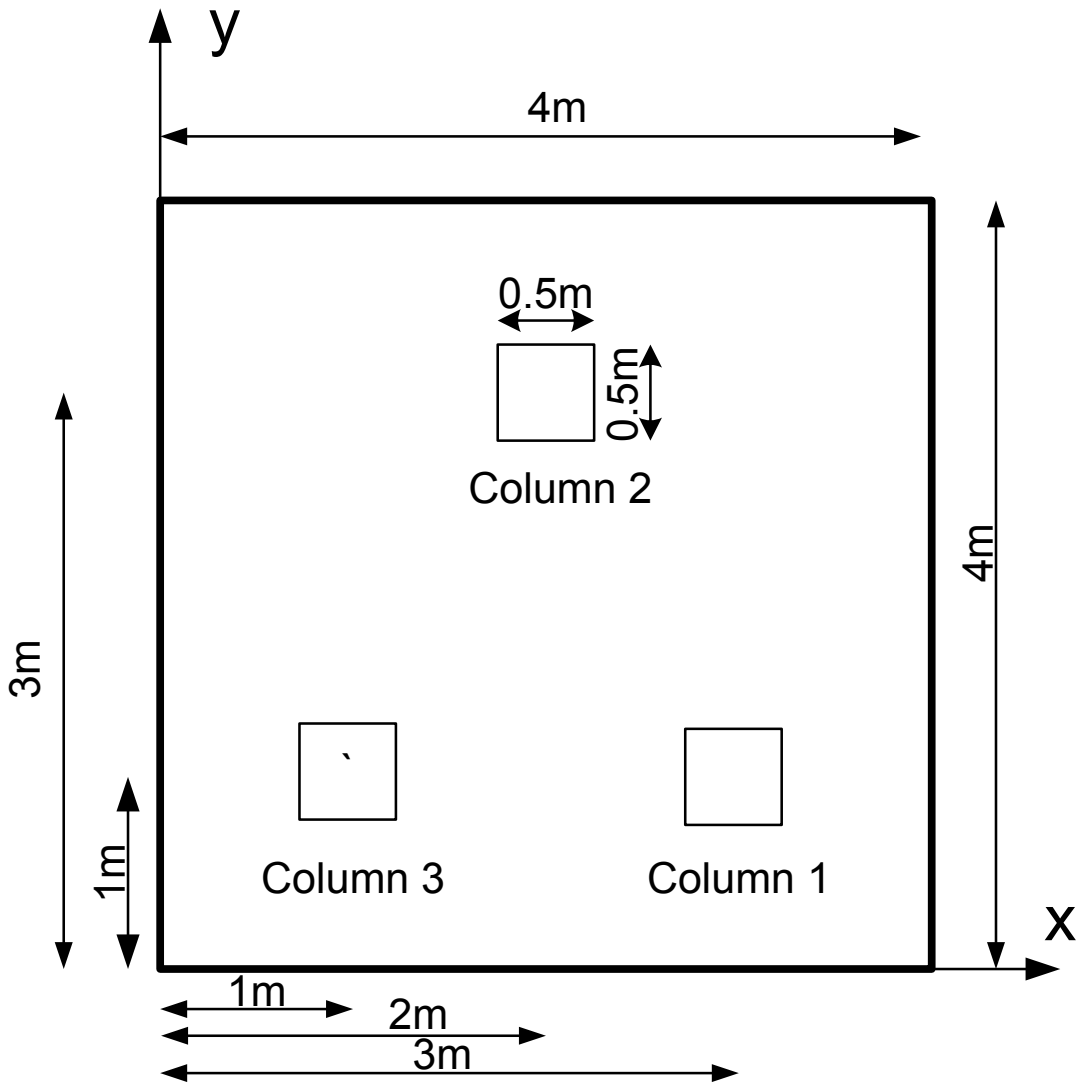


Figure 5-1: Dimensions considered for the slab in example (5.1).

The following numerical models are considered:
Model1: Considers the proposed method. The boundary element method is used to model slabs using continuous quadratic elements with element length of 1m as shown in Figure 5-2.
Model2: Considers columns as 3D solid finite elements with mesh of size 0.0625m. The slab is modeled using plate bending elements with a mesh size 0.0625m.A diaphragm constraint is enforced at the floor level as shown in Figure 5-3.
Model3: Considers columns as skeletal frame elements. The slab is modeled using the plate bending elements with a mesh size of 0.0625m. A diaphragm constraint at the floor level is enforced as shown in Figure 5-4.
It has to be noted that, in models 1 and 2 the Straus7 software [19] to carry out the finite element analysis.

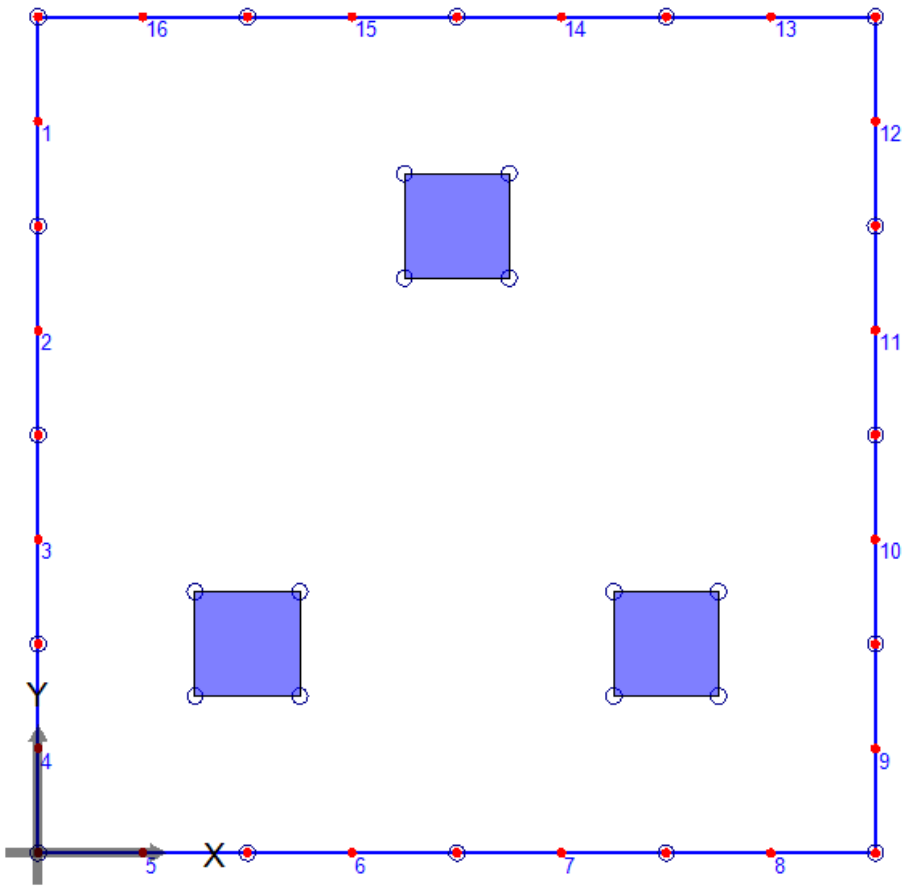


Figure 5-2: Boundary element model (model 1).

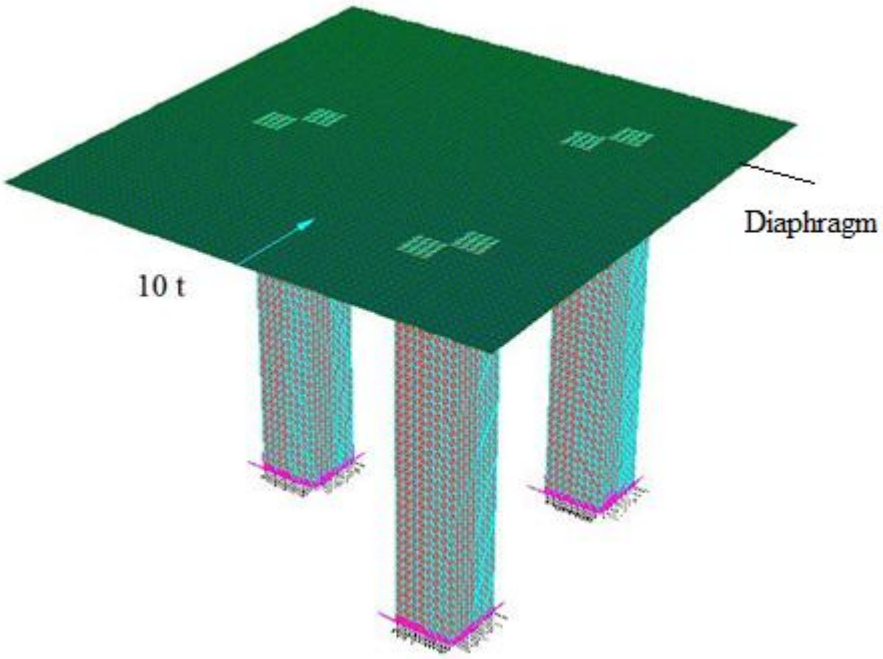


Figure 5-3: Solid element column model with slab plate bending finite element method (model 2).

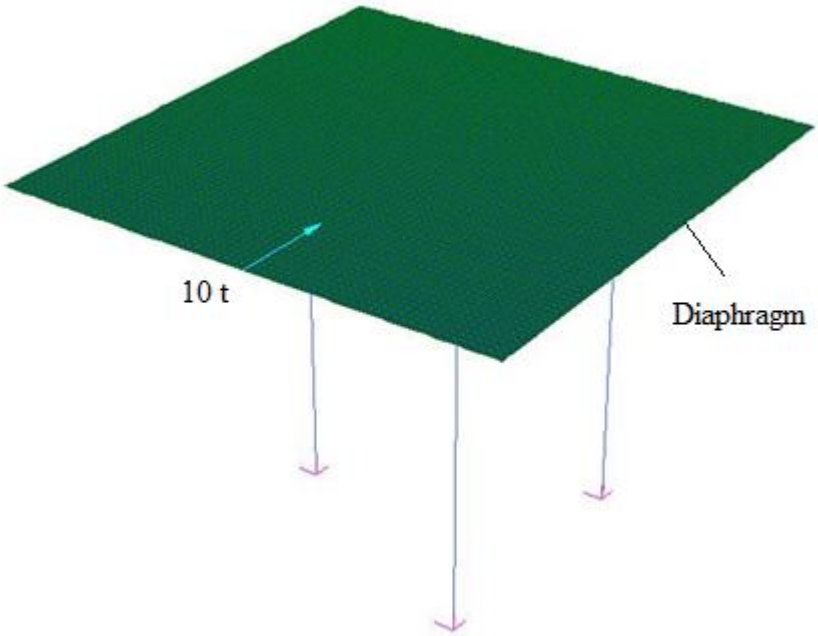


Figure 5-4: Frame element column model with slab plate bending finite element model (model 3).

Figure 5-5Figure 5- to Figure 5-7 demonstrate the bending moment a contour map and strips for the three models. In order to compare the results, Figure 5-8 demonstrates the same strip results for the three models together. It can be seen that the frame model (the common model that is used in practice of structural engineering) produces

peaking values for bending moments above support elements. If model 3 results are eliminated from 5-8, then Figure 5-9 is obtained. It is clear that the preset solution (model1) is as accurate as the (model2) in which columns are modeled as solid elements.

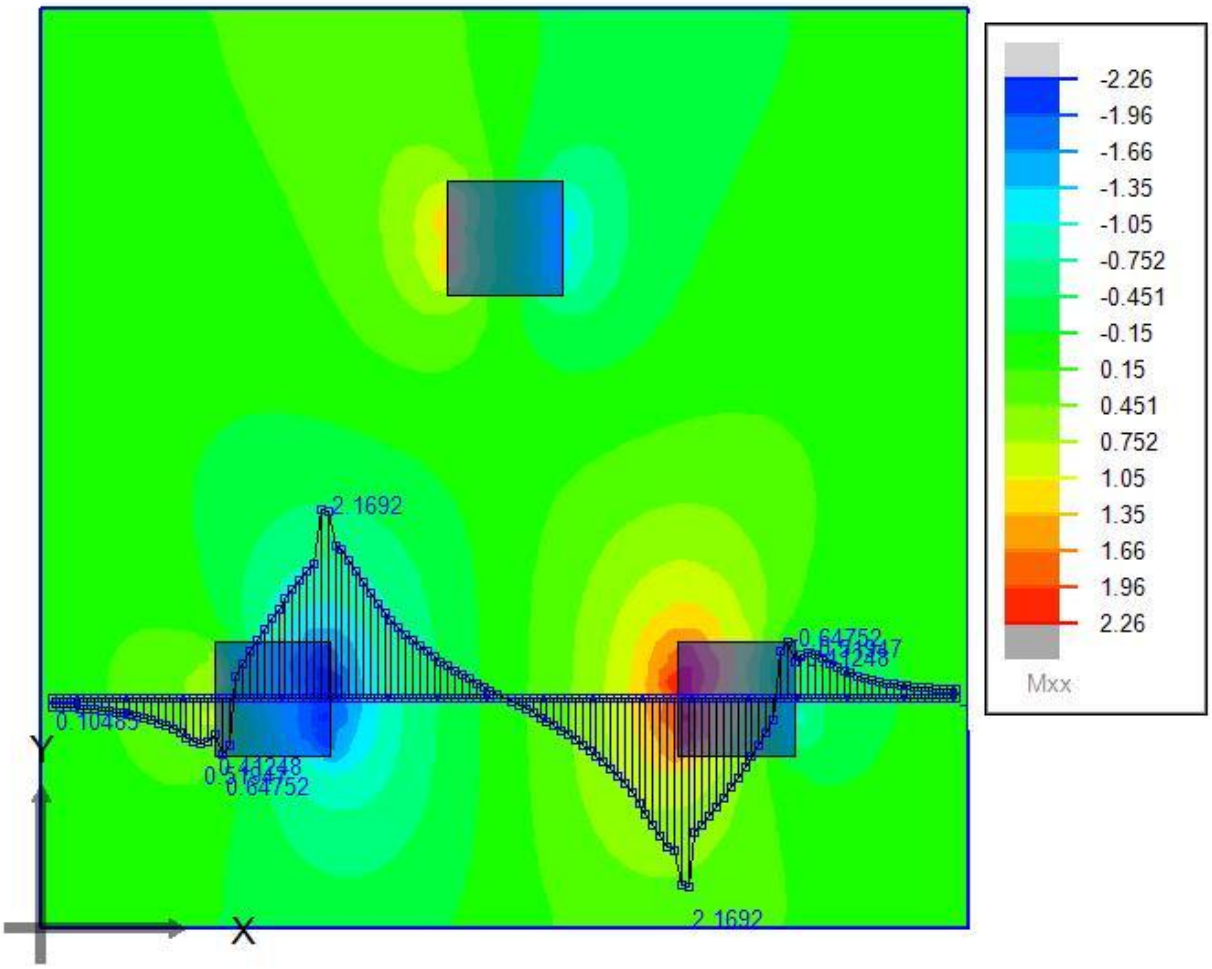


Figure 5-5: Bending moment Mxx contour in model 1.

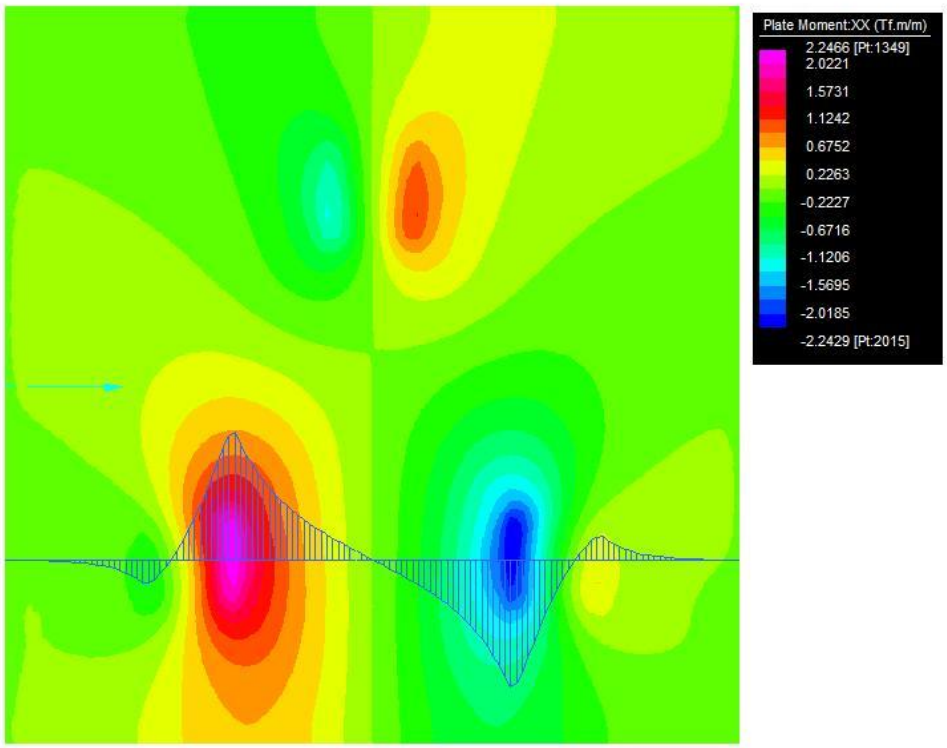


Figure 5-6: Bending moment Mxx contour map in the finite element model 2.

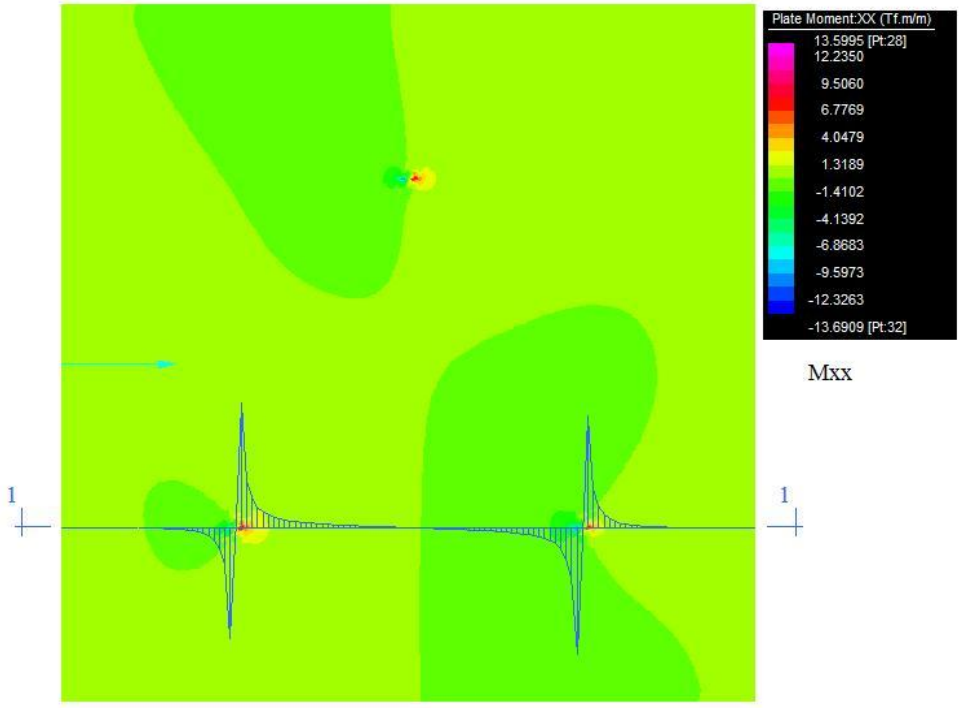


Figure 5-7: Bending moment Mxx contour map in the finite element model 3.

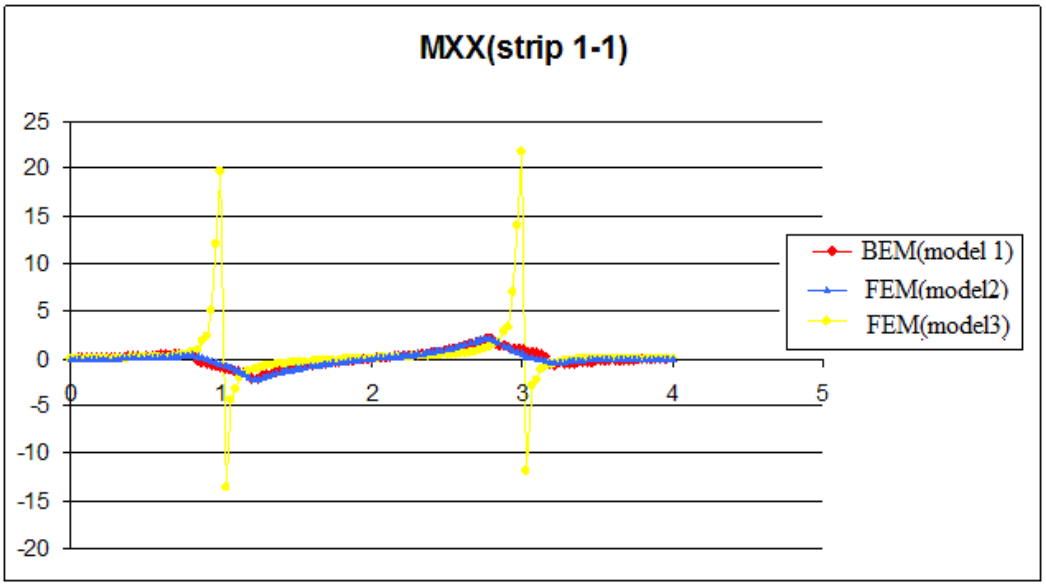


Figure 5-8: Comparison of bending moment Mxx for the considered three models.

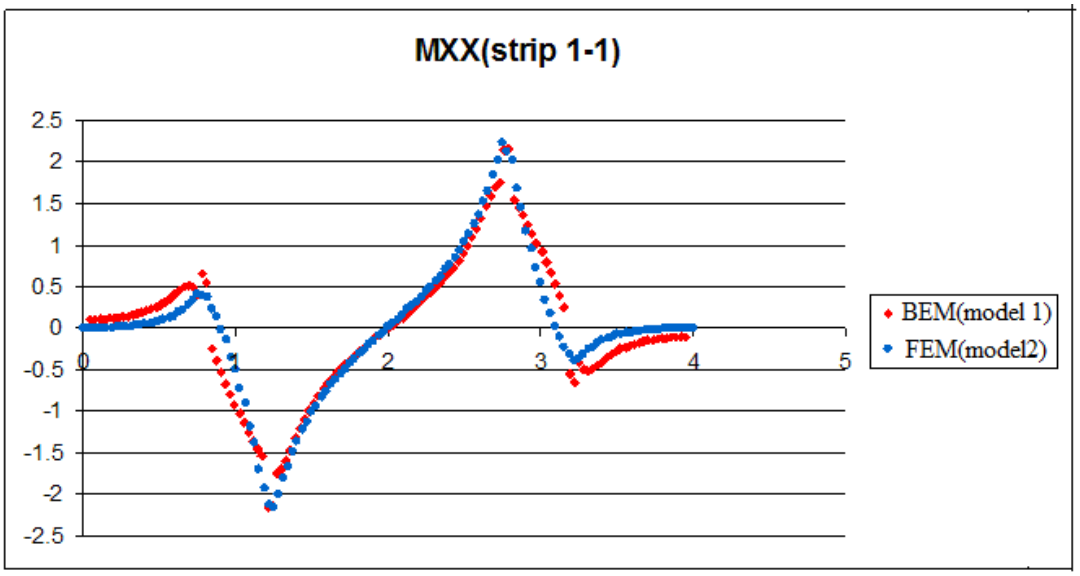


Figure 5-9: Comparison of bending moment Mxx for the considered two models.

In order to demonstrate the effect of consideration of real geometry of slab-column connection area, the following parametric study is carried out. The same example is re-considered but with 20 stories. The applied load is applied at the top floor only (floor no. 20). Two BEM models are considered, whereas the first model considered the actual connection area of columns and slab (0.5×0.5cm), whereas the second model considers the connections area between the slab and the column as a set to 10×10 cm with preserving the column stiffness properties a 0.5×0.5cm column. The drift results of the two models are demonstrated and compared to the FEM frame model (model3). It has to be noted that only the FEM model 3 is considered herein as

it is difficult to run a 20 story building with solid elements using the currently used personal computers. It can be seen from 5-10 to Figure 5-12 that both the FEM model3 and the present BEM of the 10×10cm connecting area give similar results. That means that the contact area between the slab and the column is effect in the total drift of the structural.

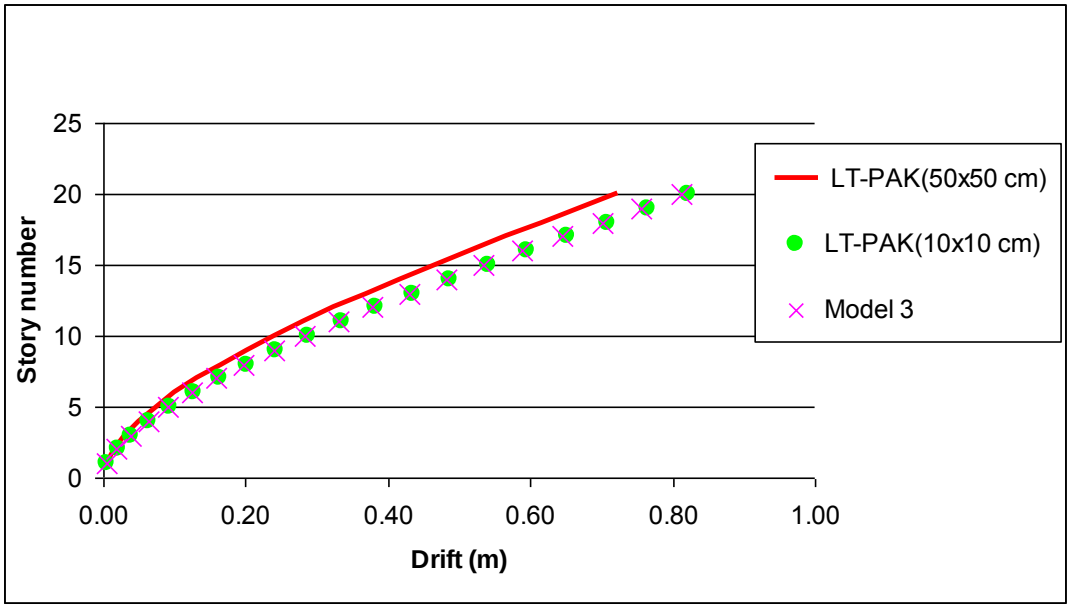


Figure 5-10 Drift in x axis.

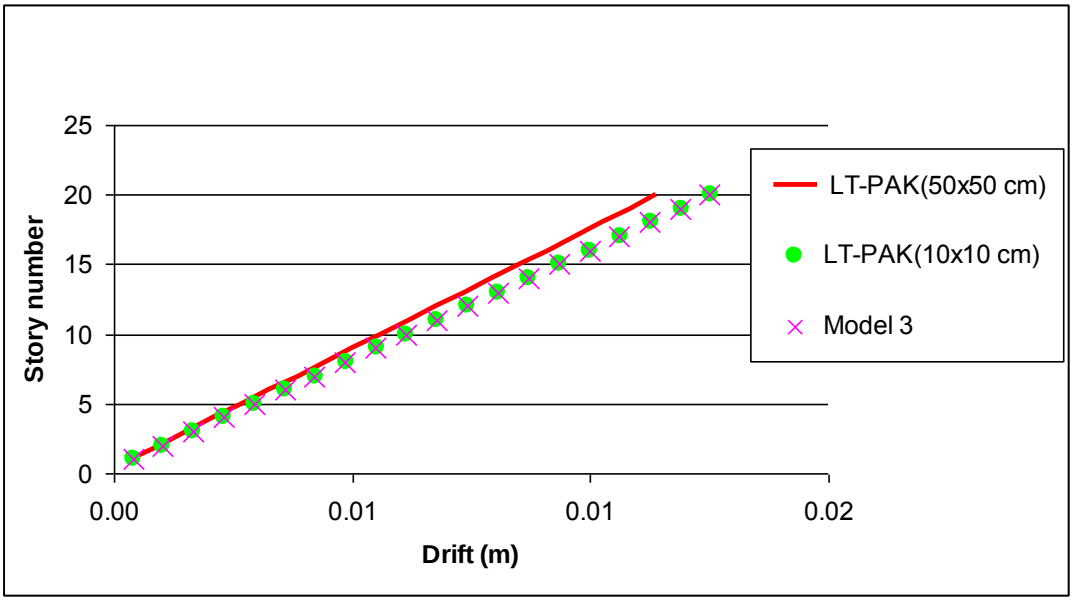


Figure 5-11 Drift in Y axes.

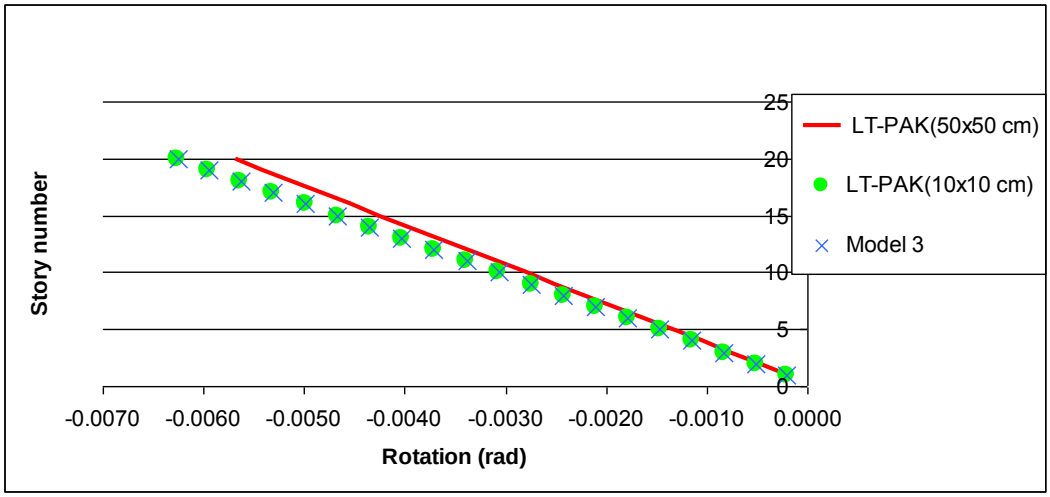


Figure 5-12 Rotation about Z axes.

## 5.2 Example (6): Practical Multi-Story Building

The purpose of this example is to demonstrate the capability of the present formulation to solve practical buildings. A 10 storey building is analyzed using the proposed method and the results are compared to those obtained from with the finite element method. The slab shown in Figure 5-13 is analyzed. It has a thickness of 0.23 m. Both the slab and vertical element materials have a modulus of elasticity equal to 2210000t/m2 and Poisson's ratio equal to 0.2. he height of each storey is 3.4m. A (1000 t) load is applied in the X-direction as show in 5-14 at all levels of the slabs. The boundary element mesh and associate discretization are shown in 5-15. The used finite element mesh is shown in 5-16, 5-17 with shell elements of size 0.5m. Columns are modeled using frame elements. A diaphragm constraint is applied at each floor level. The deflection of top slab as contour maps as shown in 5-18 and 5-19. Figures 20-26 demonstrate comparisons of deflections and lateral drifts.

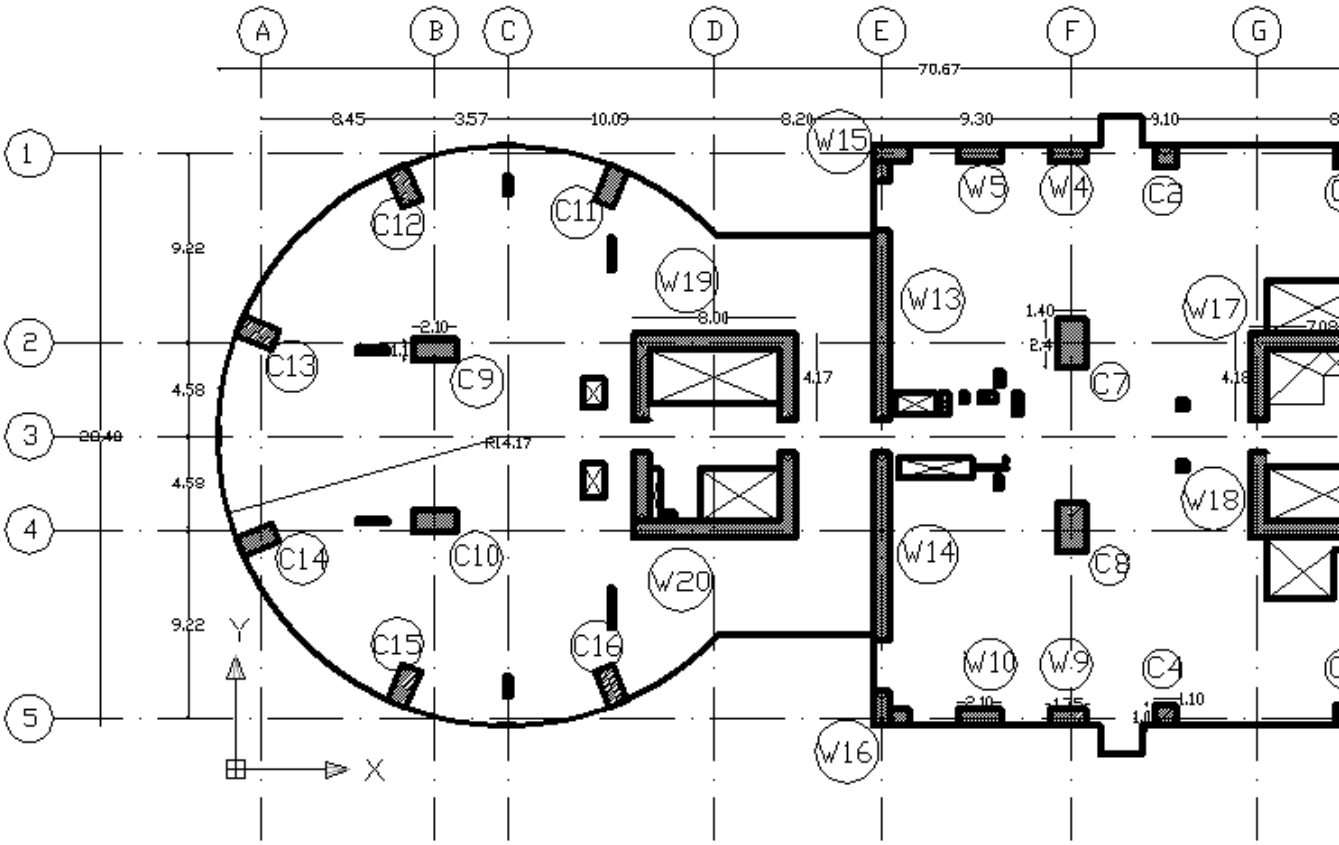


Figure 5-13: Dimensions of the Practical Building in example 5.2.

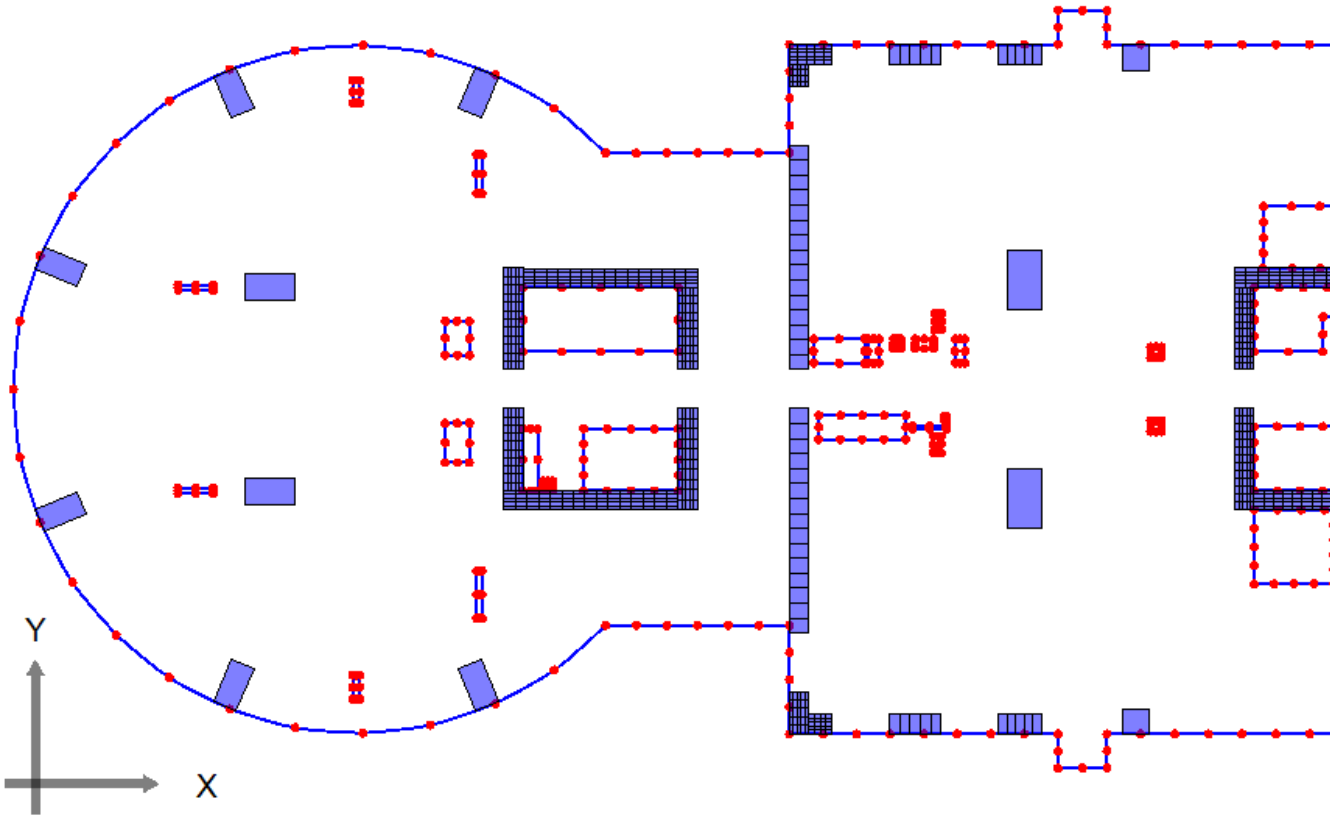


Figure 5-14: The used boundary element model in example 5.2.

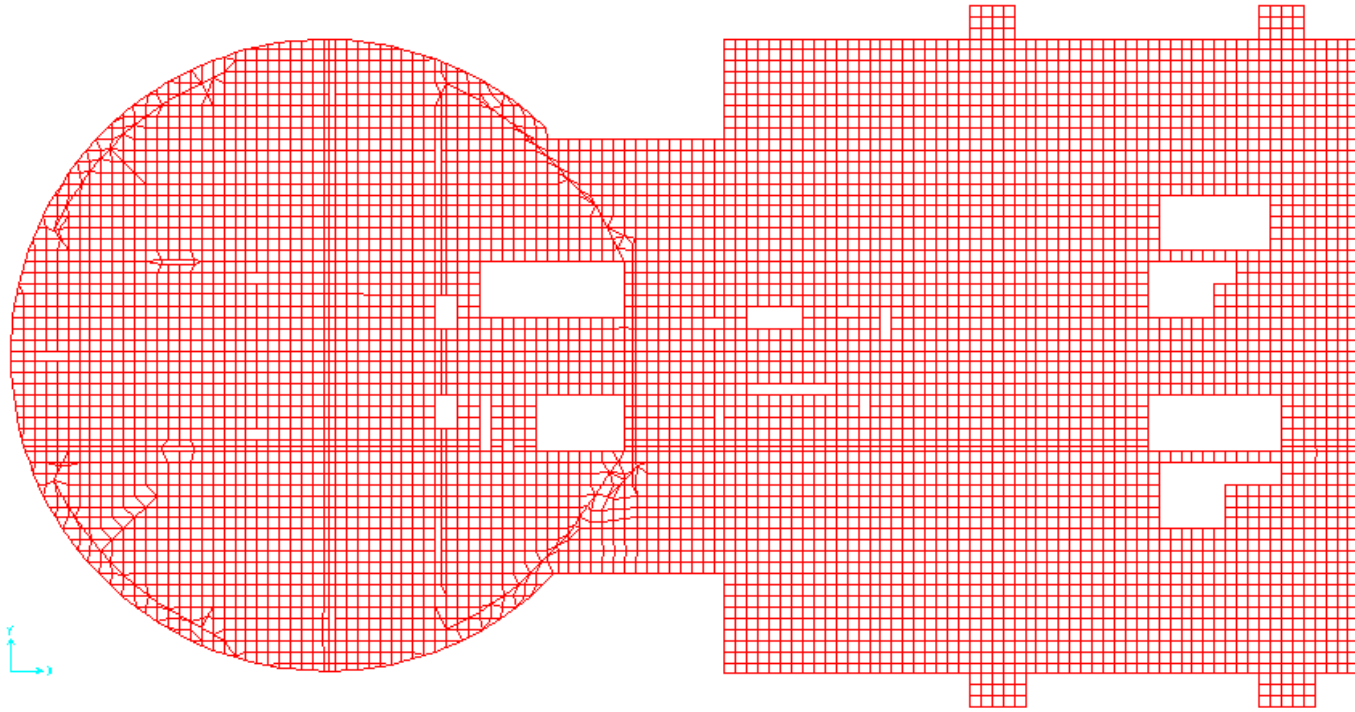

Figure 5-15: The finite element mesh used in example 5.2.

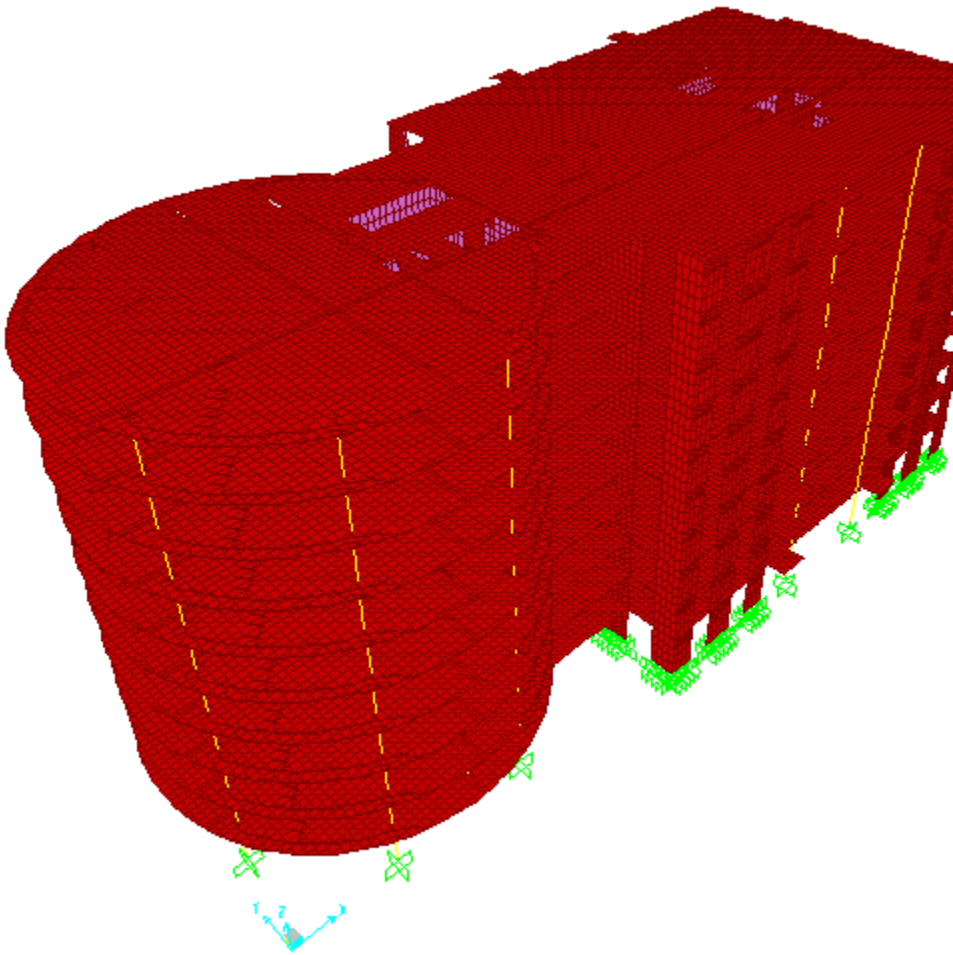

Figure 5-16: The multi-storey finite element model in example 5.2.

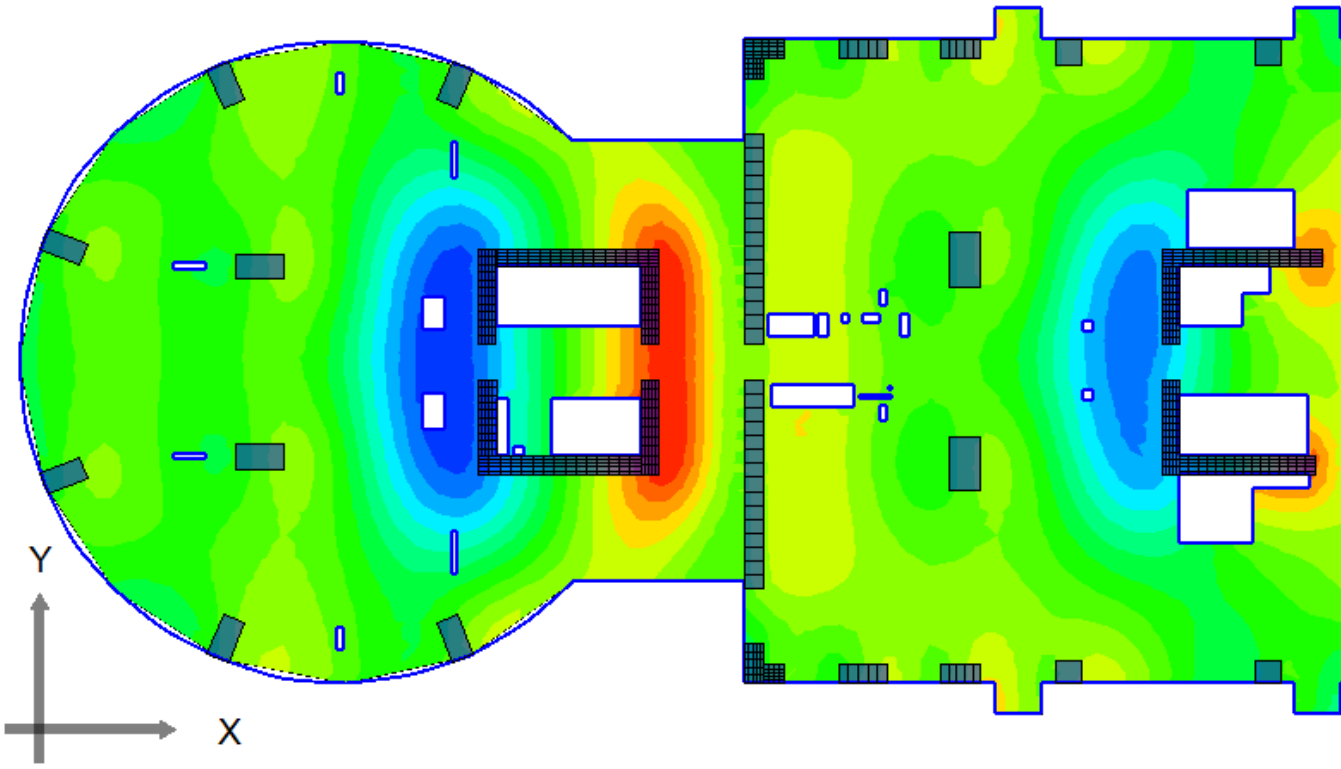


Figure 5-17 Slabs deflection UZ _BEM_Model (1).

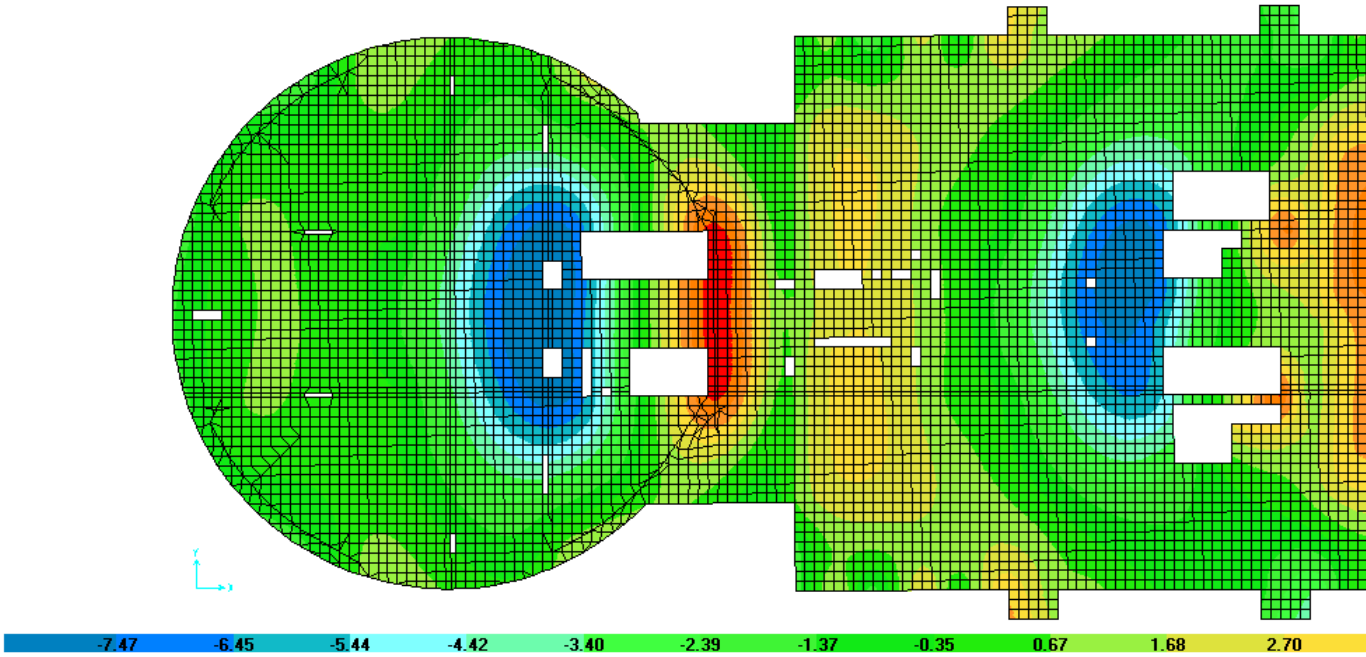


Figure 5-18: Slabs deflection UZ- FEM-Model (2).

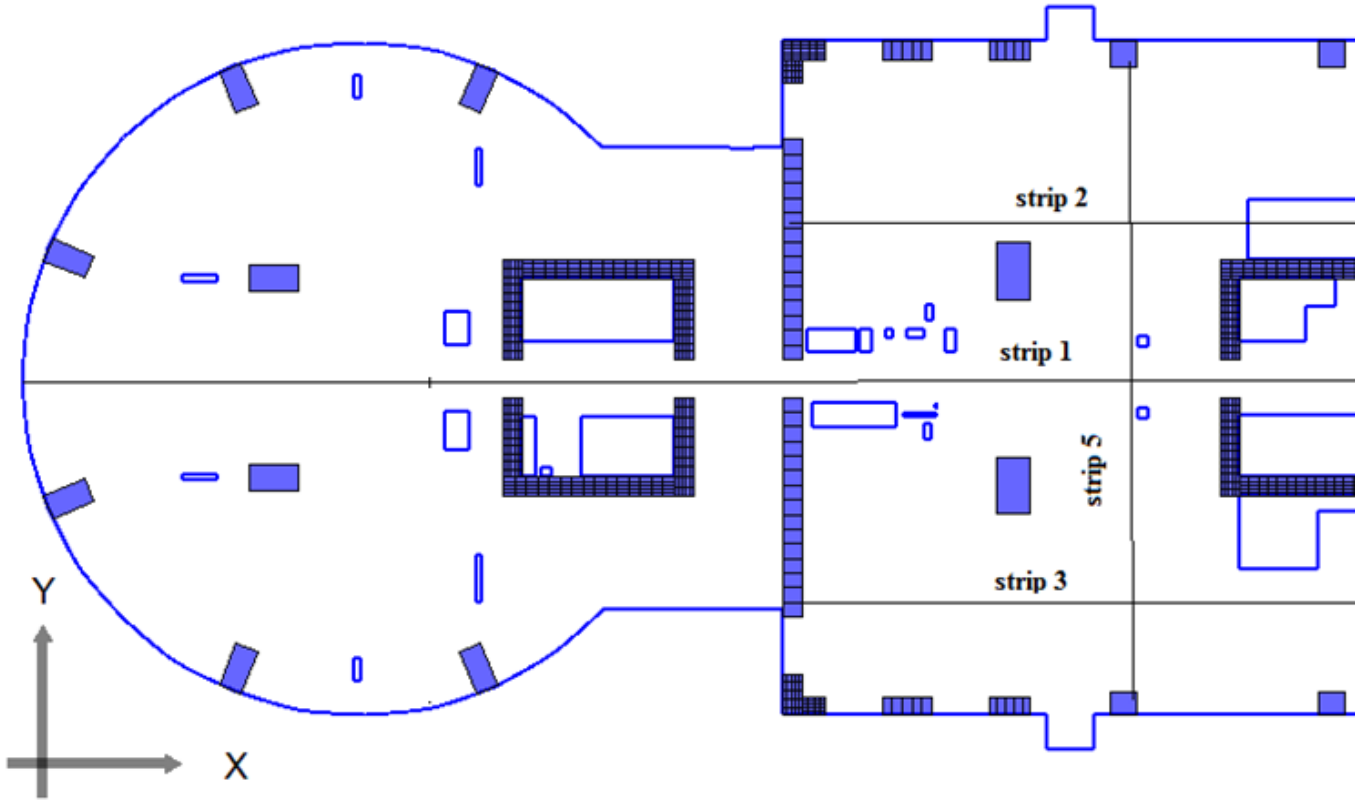


Figure 5-20: Strip guide

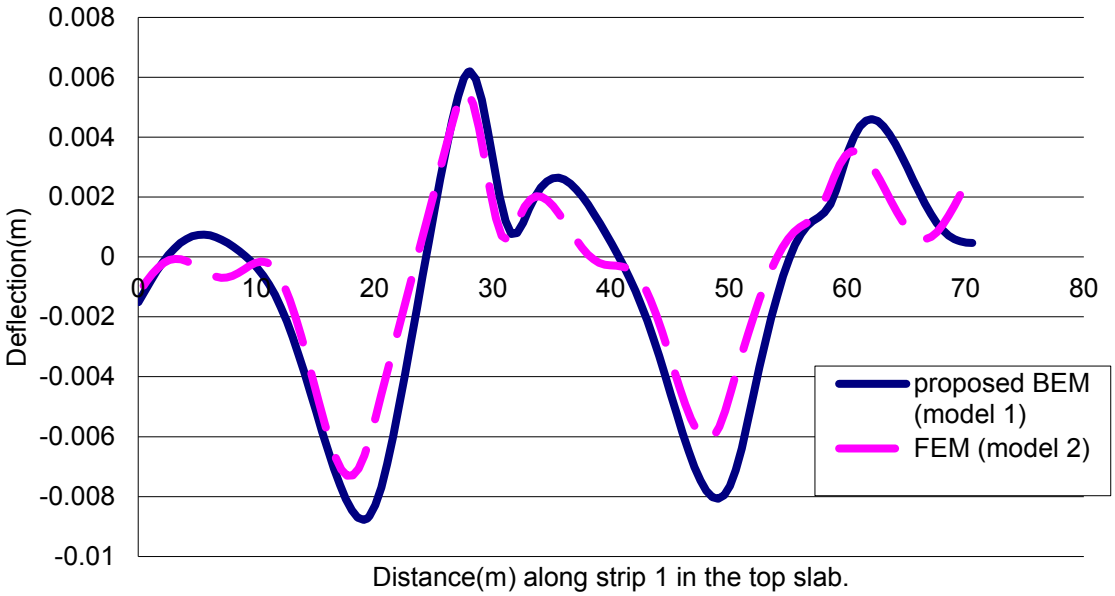


Figure 5-21: Comparison of deflection UZ diagram between two models strip 1.

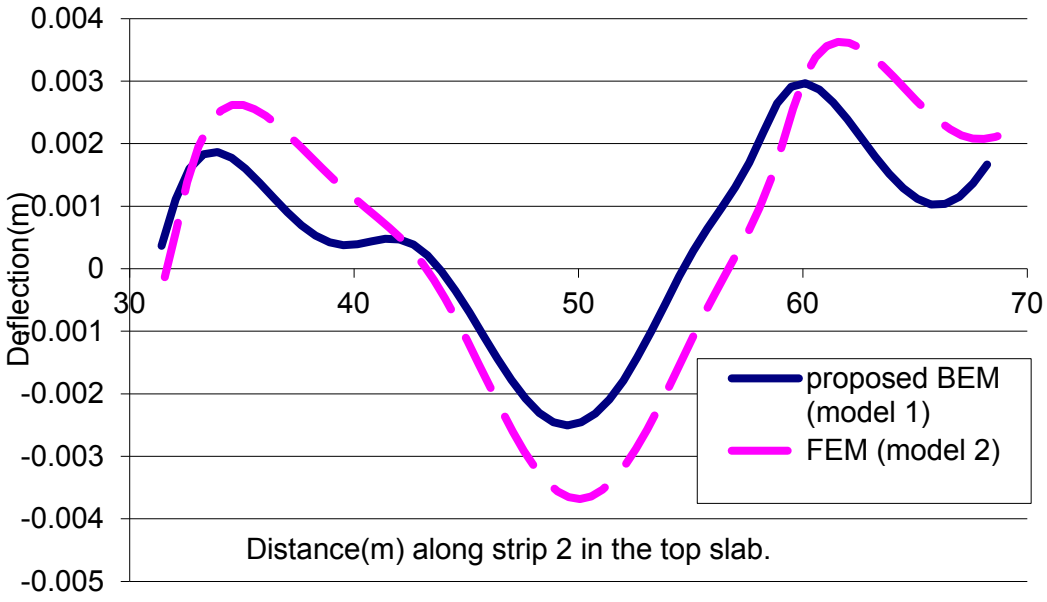


Figure 5-22 Comparison of deflection UZ diagram between two models strip 2.

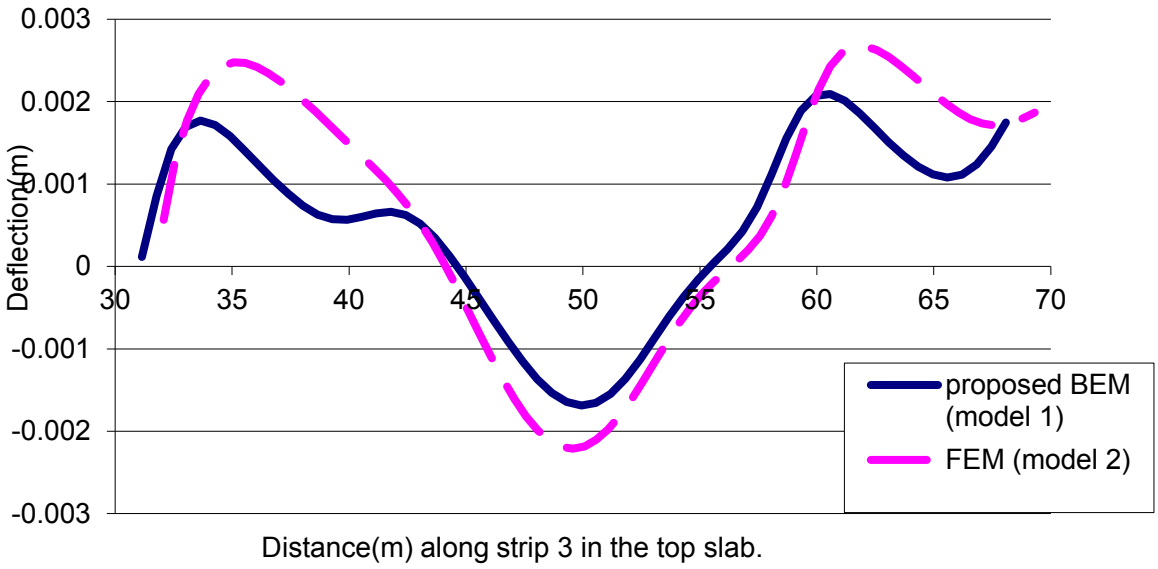


Figure 5-23 Comparison of deflection UZ diagram between two models strip 3.

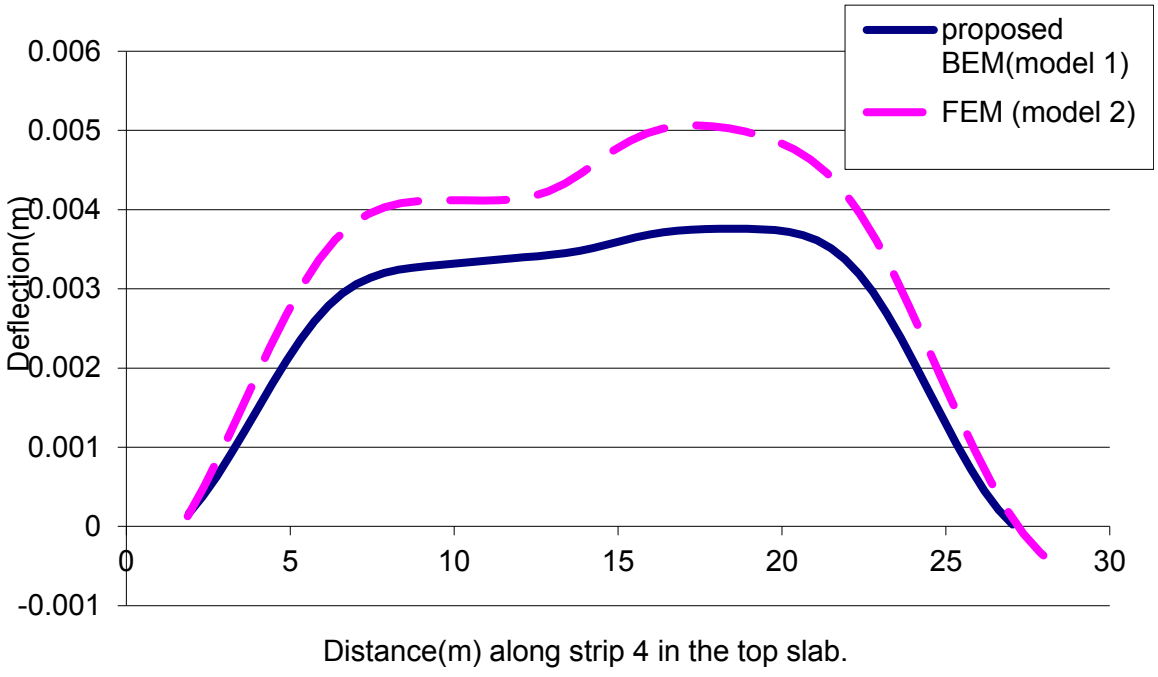


Figure 5-24 Comparison of deflection UZ diagram between two models strip 4.

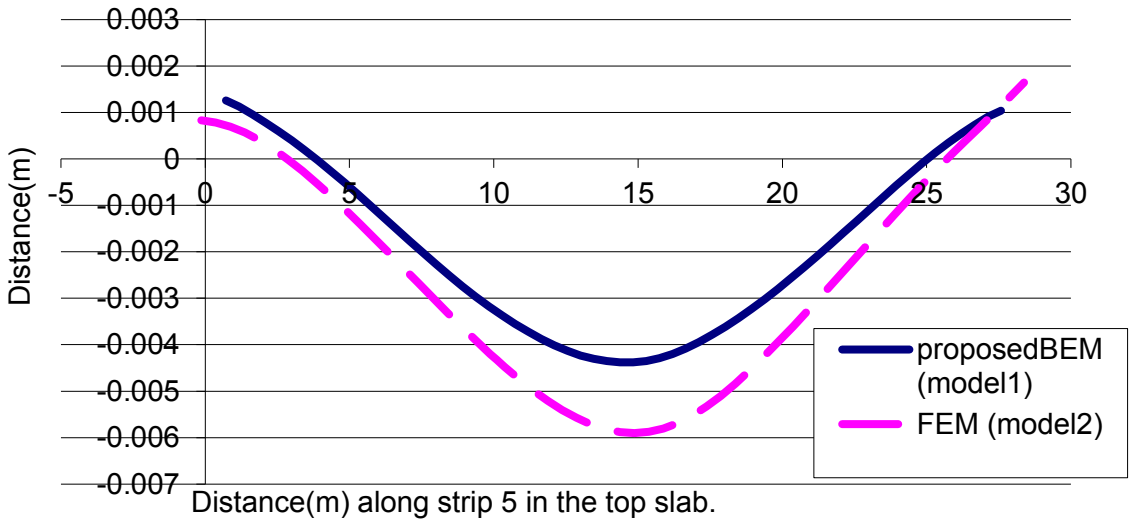


Figure 5-25 Comparison of deflection UZ diagram between two models strip 5.

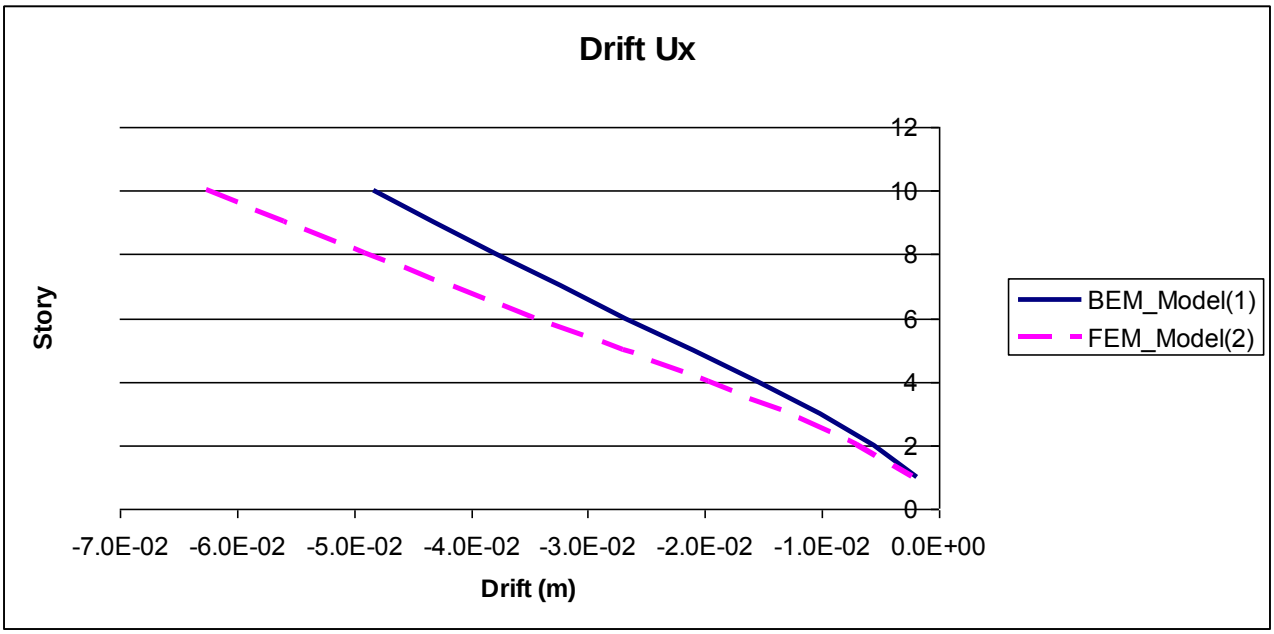


Figure 5-26: Comparison of lateral drifts in X direction.

## 6 CONCLUSIONS

This paper presents a new scheme for the lateral analysis of buildings using matrix analysis of structures. In the presented scheme, the stiffness matrices of vertical elements are computed; including the warping effects for large wall sections. The stiffness matrices of plate elements are computed using a boundary element formulation; the stiffness co-coefficients are condensed at vertical elements positions. The proposed scheme is applied to a couple of examples. The first one demonstrates the significance of the real geometry modeling presented by the

proposed boundary element modeling. The second demonstrates the applicability of the proposed scheme to practical applications.

## ACKNOWLEDGMENT

The research reported here was supported by the European Union Project PIRSES-GA-2010-269222: Analysis and Design of Earthquake Resistant Structures (ADERS) of the FP7-PEOPLE-2010-IRSES, Marie Curie Actions. This support is gratefully acknowledged by the authors.

## REFERENCES

[1] B., S. a ranath "Structural analysis and design of tall buildings," New York, McGraw-Hill, 1988.

[2] B. S. Smith and A. Coull, 'Tall Building Structures Analysis and Design, Tall' Buildings Structures-Analysis and Design, John Wiley & sons Publication.

[3] O.C., Zienkiewicz, 'The finite element method' McGraw Hill, 1977

[4] A. Ghali, A.M. Neville and .G . Brown 'structural analysis a unified classical and at ri approach 6th edition' by a ylor&francis Publication, Chapter 14 PP 417-428.

[5] H.C ,Chan, YK.,Cheung 1979. Analysis of shear wall using higher order finite elements. Building and Environment 14(3): 217–224.

[6] R., Rosman 'Statics of non-sy etric shear wall structures' Proceedings of the Institution of Civil Engineers 48–49(Suppl 12): 211–244, 1971.

[7] JK,Biswas WK. ,Tso 1974. 'Three-dimensional analysis of shear wall buildings to lateral load'. Journal of the Structural Division, Vol. 100, No. 5, 5,1974

[8] J ,Wdowicki, E, Wdowicka. 1993b. System of programs for analysis of three-dimensional shear wall structures. The Structural Design of Tall Buildings Vol. 2 ,1993.

[9 Jacek Wdowicki and Elz˙bieta Wdowicka Analysis of shear wall structures of variable cross section Structrl. Design Tall Spec. Build, 2012.

[10] A,Coull, RD , Puri. ‘Analysis of coupled shear walls of variable thickness’ Building Science , 1967

[11] A,Coull, RD , Puri. ‘Analysis of coupled shear walls of variable cross-section. Building Science, 1968.

[12] A. Pisanty, EE, Traum. ‘Si plifi ed analysis of coupled shear walls of variable cross-section’ Building Science, 1970

[13] O, Aksogan, HM, Arslan, BS, Choo.’Forced vibration analysis of stiffened coupled shear walls using continuous connection method’ Engineering Structures, 2003

[14] Y.F.Rashed, "Boundary element Modeling of flat plate floors under vertical loading", Int. J. Numer. Meth. Engng. Vol. 62:1606-1635,2005.

[15] E. Reissner, "On the theory of bending of elastic plates", Journal of Mathematics and Physics, Vol. 23, pp.184-191,1944.

[16]E.Reissner, "On bending of elastic plates", Quart. Applied Mathematics, Vol. 5, pp. 55-68,1947.

[17 Vlasov, Vasili Zakharovich , “ hin -walled elastic bea s “2. ed. rev. and augm. Tranl. From Russian,1906-1958.

[18] J. T. Katsikadelis ‘boundary ele e nts theory and applications’ by Elsevier science Ltd.2003.

[19] Sraus7 finite element analysis system –www.strand7.com.